Optics Letters

Continuously tunable single-frequency 455 nm blue laser for high-state excitation transition of cesium

Fengqin Li,[1,2,3] Biao Zhao,[1] Jiao Wei,[1] Pixian Jin,[1,2] Huadong Lu,[1,2,*] and Kunchi Peng[1,2]

[1]State Key Laboratory of Quantum Optics and Quantum Optics Devices, Institute of Opto-Electronics, Shanxi University, Taiyuan 030006, China
[2]Collaborative Innovation Center of Extreme Optics, Shanxi University, Taiyuan, Shanxi 030006, China
[3]e-mail: lfq@sxu.edu.cn
*Corresponding author: luhuadong@sxu.edu.cn

Received 28 June 2019; revised 4 July 2019; accepted 4 July 2019; posted 5 July 2019 (Doc. ID 371286); published 24 July 2019

A continuously tunable high-power single-frequency 455 nm blue laser for high-state excitation transition $6^2S_{1/2}\leftrightarrow 7^2P_{3/2}$ of Cs atoms was presented in this Letter, which was implemented by an intracavity frequency-doubled Ti:sapphire laser with an LBO crystal. The highest output power of 1.0 W was attained under a pump power of 13.5 W with an optical conversion efficiency of 7.4%. The measured power stability in 3 h and beam quality were better than ±0.27% (peak-to-peak) and $M_x^2 = 1.58$, $M_y^2 = 1.18$, respectively. By continuously scanning the length of the resonator after locking the employed intracavity etalon to the oscillating longitudinal mode of the laser, the continuous tuning range of the 455 nm blue laser was up to 32 GHz and was mode hop free. Lastly, the whole saturation absorption spectrum of the higher state excitation transition $6^2S_{1/2}(F_g = 3)\leftrightarrow{}^2P_{3/2}(F_e = 2, 3, 4)$ and $6^2S_{1/2}(F_g = 4)\leftrightarrow 7^2P_{3/2}(F_e = 3, 4, 5)$ of ^{133}Cs was successfully observed in the experiment, which further verified the excellent performance of the 455 nm blue laser. © 2019 Optical Society of America

https://doi.org/10.1364/OL.44.003785

Single-frequency continuous-wave (CW) 455 nm lasers are an important source for a great deal of fields, including high-resolution and precision spectroscopy, optical frequency standards and clocks, special atomic interferometry and manipulations, quantum optics and quantum information, and so on [1–3]. Especially, they can act as the pump laser to measure the lifetime or the hyperfine structure parameters of cesium (Cs) atom states with the natural linewidth of 1.2 MHz [4] or realize a Cs atomic resonance filter (ARF) with high transmission (HT) and ultranarrow bandwidth in underwater communications [5], since the wavelength of 455 nm was just corresponding to the higher state excitation transition ($6^2S_{1/2}\leftrightarrow 7^2P_{3/2}$) of Cs atoms. In order to implement precise measurement and achieve long-distance undersea communication, it was necessary to effectively increase the output power of the single-frequency 455 nm blue laser and achieve accurate frequency tuning for matching the higher state excitation transition of Cs atoms. However, it was factually difficult to achieve this goal because there was not a suitable laser crystal that was up to this task. Schmidt *et al.* reported a 455 nm laser by using a new Nd:$LiLuF_4$ crystal and an LBO as the gain medium and second-harmonic generator in 2001, but the output power of the 455 nm laser was restricted to 40 mW, which resulted from its poor emission cross section 2×10^{-20} cm^2 and thermal conductivity [6]. A CW single-frequency 455 nm blue laser was also realized with an external frequency-doubled diode laser [7]. However, it was necessary to employ an amplifier to amplify the power of the diode laser, which can complicate the structure of the laser system. Even so, the output power of the CW single-frequency 455 nm laser was still restricted less than 300 mW. In contrast to the previous research, the Ti:sapphire (Ti:S) crystal can be a perfect candidate because its fluorescence spectrum range not only can extend from 700 to 1000 nm but the emission cross section of the covered wavelength of 911 nm and thermal conductivity were also as high as 1.9×10^{-19} cm^2 and 0.33 W/(cm · K), respectively. In 2007, Cruz *et al.* compared the external frequency-doubling to the intracavity frequency-doubling Ti:S laser and concluded the conversion efficiency from the green pump to the blue laser could be increased with intracavity frequency doubling of the Ti:S laser [8]. However, the output power of single-frequency 423 nm blue laser was still restricted to 266 mW, which resulted from the large loss of the intracavity optical diode. In 2016, our group demonstrated a single-frequency CW 455 nm laser with the output power of 421 mW by an intracavity-doubling Ti:S laser with a BIBO crystal [9]. The disadvantage of the upper threshold pump power due to the smaller gain at the oscillating wavelength of 911 nm was overcome by optimizing the parameters of the resonator. Unfortunately, the output beam quality of the blue laser was imperfect because of the serious walk-off effect of the frequency-doubling BIBO crystal. And, the continuous tuning range was limited to be 3.4 GHz, only depending on the nonlinear loss in the cavity, which can partially scan the saturation absorption spectrum (SAP) of the high-state excitation transition $6^2S_{1/2}(F_g = 4)\leftrightarrow 7^2P_{3/2}(F_e = 3, 4, 5)$ of ^{133}Cs.

Even so, it paved a good way to realize a CW tunable single-frequency 455 nm laser for the high-state excitation transition of cesium. In this Letter, we report a single-frequency intracavity frequency-doubled CW 455 nm Ti:S laser with an LBO crystal, which had a smaller walk-off angle than BIBO crystal. The output power of the single-frequency 455 nm blue laser can reach up to 1.0 W. To the best of our knowledge, that is the highest achieved output power at the wavelength of 455 nm. Especially, after locking the employed intracavity etalon (IE) to the oscillating longitudinal mode of the laser by a direct modulation-locking method, the continuous frequency-tuning range can reach up to 32 GHz around 455.528 nm, which was enough for the high-state excitation transition $6^2S_{1/2}\leftrightarrow 7^2P_{3/2}$ of Cs atoms. Eventually, using the attained 455 nm laser, the whole SAP of the higher state excitation transition $6^2S_{1/2}(F_g = 3)\leftrightarrow 7^2P_{3/2}(F_e = 2, 3, 4)$ and $6^2S_{1/2}(F_g = 4)\leftrightarrow 7^2P_{3/2}(F_e = 3, 4, 5)$ of ^{133}Cs was successfully obtained from the interaction between the 455 nm laser and the ^{133}Cs atom gas.

The schematic of the designed single-frequency CW 455 nm laser was depicted in Fig. 1. A homemade single-frequency CW 532 nm green laser with an output power of 13.5 W acted as the pump source [10,11]. The green laser beam was transformed by a telescope system composed of two lenses with focal lengths of 150 mm and 85 mm, respectively, and injected into the laser resonator. A half-wave plate (HWP) at 532 nm in front of the resonator was used for the polarization alignment. The gain medium was a Brewster-cut (60.4°) Ti:S crystal with a length of 20 mm and diameter of 4 mm, respectively. The Ti^{3+}-doped concentration was 0.05 at wt. %, which was corresponding to the absorption coefficient of 1.13 cm^{-1} at 532 nm. In order to increase the optical conversion of the designed laser, the Ti:S crystal was mounted in a water-cooled copper oven, and the temperature of the Ti:S crystal was controlled to be 16.5°C. In order to create two tightly focused beam waists for placing the Ti:S and frequency-doubling crystal in one cavity, an embedded six-mirror ring resonator consisting of two pairs of concave mirrors M_1, M_2 and M_4, M_5 and two flat mirrors M_3, M_6 was constructed. The curvature radii of all of the concave mirrors were 75 mm. Input coupler (IC) M_1 was a meniscus concave mirror and coated with HT film at 532 nm ($T > 95\%$) and high-reflection (HR) film at 911 nm ($R > 99.9\%$). Output coupler (OC) M_4 was coated with HR film at 911 nm ($R > 99.9\%$) and HT film at 455.5 nm ($T > 95\%$). The other mirrors M_2, M_3, M_5, and M_6 were all coated with HR film at 911 nm ($R > 99.9\%$). For all of the HR films, the coating bandwidth was ±20 nm, which could effectively suppress the oscillation of the gain peak of 795 nm and ensure that the oscillating laser wavelength was near 911 nm. Two piezoelectric transducers (PZT_1 and PZT_2, Piezomechanik GmbH) with lengths of 15 mm were successively glued to M_3 and M_6 for fine scanning. Incident angles of M_1, M_2 and M_4, M_5 were set to 18° and 4°, respectively, for compensation of the astigmatism introduced by the Brewster faces and thermal lens of the Ti:S crystal. The frequency-doubling crystal used in our experiment was a I-type phase-matching LBO crystal with a length of 7.5 mm, which was placed between M_4 and M_5. Both ends of the LBO crystal were coated with antireflection (AR) films at 911 and 455.5 nm. The operating temperature of the LBO crystal was controlled to be 30.90°C by a homemade temperature controller with a high precision of 0.01°C. To enforce unidirectional oscillation of the designed laser, a broadband optical diode consisting of a Brewster-cut TGG Faraday crystal with a length of 3.5 mm and a thin quartz crystal with a thickness of 0.334 mm was inserted into the cavity. A three-plate quartz birefringent filter (BRF) with thicknesses of 1, 2, and 4 mm was employed to implement the coarse frequency tuning. A fused silica IE with a thickness of 0.5 mm and diameter of 10 mm was adopted to narrow the linewidth and realize the fine frequency tuning of the laser. In order for mode selectivity and development of the continuous tuning range of the laser, the adopted IE was coated with a partial reflectivity of 20% at the oscillating wavelength of 911 nm. In the experiment, the wavelength of the designed laser was monitored by a wavelength meter (WLM, WS6, High finesse) with a precision of 0.0001 nm.

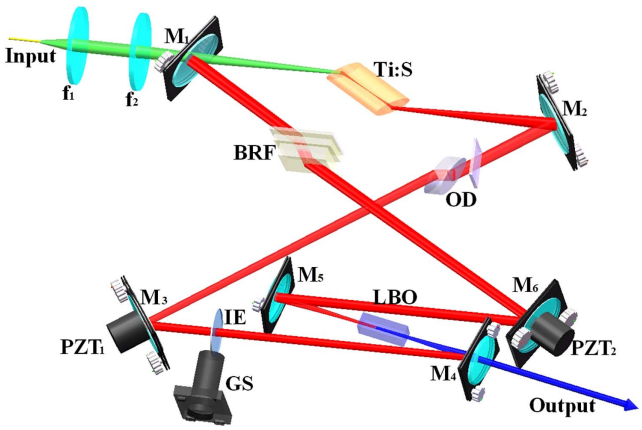

Fig. 1. Schematic of the continuously tunable single-frequency CW 455 nm Ti:S laser.

In the experiment, we first rotated the optical axis of the BRF and the incident angle of the IE for tuning the operating wavelength of the fundamental wave (FW) laser to 911.056 nm. In this case, the wavelength of the second-harmonic wave laser was 455.528 nm, which was corresponding to the high-state absorption line $6^2S_{1/2}\leftrightarrow 7^2P_{3/2}$ of the Cs atoms. At this time, the output power of the achieved single-frequency 455 nm laser versus the incident pump power of the 532 nm laser was recorded and illustrated in Fig. 2(a). It revealed that the threshold pump power was 2.0 W and the maximal output power was 1.0 W under the maximal pump power of 13.5 W. The attained maximal optical–optical conversion efficiency was 7.4%. The long-term power stability was also measured and shown in Fig. 2(b). It can be known that the power stability in 3 h was better than ±0.27% (peak-to-peak), which was a benefit from the power stability of the pump source and the perfect quality of the Ti:S laser crystal. The longitudinal mode structure of the laser was also monitored by a homemade confocal Fabry–Perot interferometer with a free spectrum range and finesse of 750 MHz and 120, respectively. The transmission curve shown in Fig. 2(c) presented that the laser can stably work with single longitudinal mode operation. The beam quality M^2 of the obtained 455 nm blue laser was also measured by a laser beam profiler (M2DU, DataRay Inc.), and the measured M^2 was better than $M_x^2 = 1.58$ and $M_y^2 = 1.18$, as shown in Fig. 2(d). Though the walk-off effect of the LBO crystal was much smaller than that of other nonlinear crystals including BBO and BIBO crystals, the elongated spots were still clearly visible.

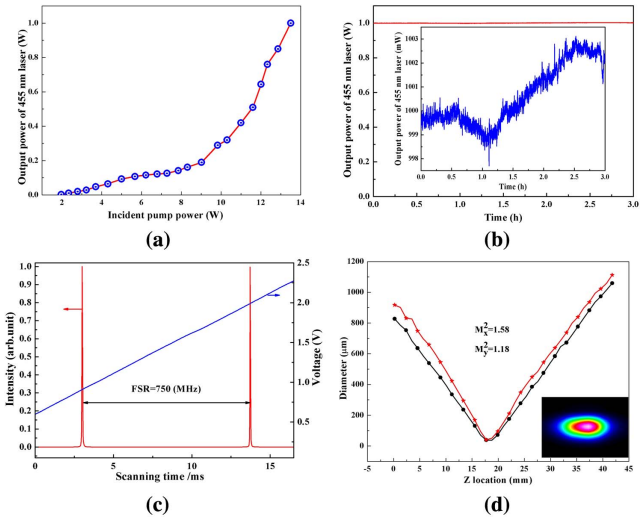

Fig. 2. Output characteristics of the single-frequency CW 455 nm laser. (a) Output power curve of the 455 nm laser versus the incident pump power, (b) long-term power stability of the 455 nm laser for 3 h, (c) the measured longitudinal mode structure, and (d) the measured beam quality M^2.

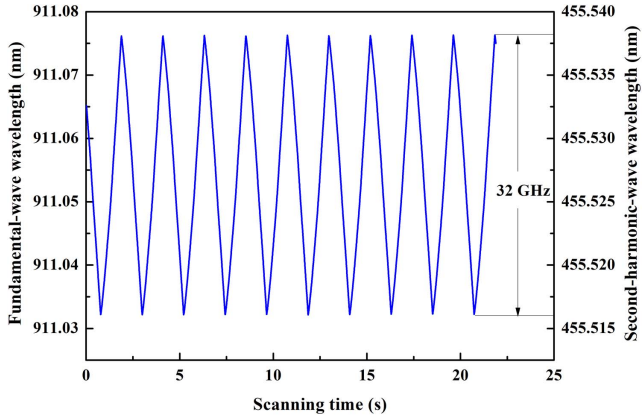

Fig. 4. Continuous frequency-tuning curve of the single-frequency CW 455 nm laser.

The measured linewidth of the 455 nm laser was 380 kHz with a delayed self-heterodyne interferometer.

In order to attain the fine and continuous frequency tuning of the designed single-frequency CW 455 nm laser that is mode hop free, the IE was first locked to the oscillating longitudinal mode of the laser by a direct modulation-locking method. Different from the traditional methods including the PZT-modulated and electro-optical effect-modulated methods, the adopted IE coated with the film of partial reflectivity ($R = 20\%$) was directly mounted on the spindle of a driven galvanometer scanner (GS), and a modulation signal was directly loaded on the driver of the GS together with the feedback signal as well as the offset voltage. Figure 3 depicted the operating diagram and the IE motion trace. According to Fig. 3(a), a small part of the leaked FW laser from the resonator was separated and detected by a photodiode (PD_1). When a sinusoidal modulation signal (Signal 1) with a frequency and amplitude of 1.3 kHz and 300 mV, respectively, generated by a function

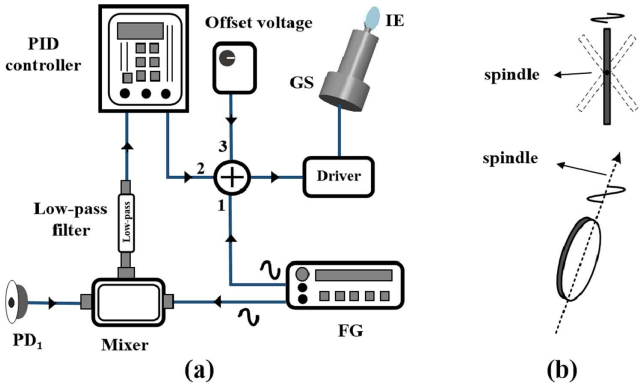

Fig. 3. (a) Schematic diagram of the servo control system for etalon-locking and (b) motion trace of the etalon.

generator (FG), was uploaded on the driver of GS, the IE could periodically swing, which is shown in Fig. 3(b), and the intensity of the intracavity laser was modulated. Another signal with the same frequency as the modulation signal and the adjustable phase as well as the amplitude of 700 mV was used to mix with the detected signal created by PD_1 for generating the error signal. The generated error signal went through a low-pass filter circuit and a proportion-integration-differentiation (PID) circuit, then the feedback signal (Signal 2) was generated and uploaded on the driver of the GS. In order to finely tune the position of the transmission peak of the IE relative to the cavity longitudinal mode, an adjustable offset voltage (Signal 3) was also added to the driver of the GS. As a result, by optimizing the amplitude and frequency of the modulation signal and precisely adjusting the offset voltage, the transmission peak of the IE was successfully locked to the cavity longitudinal mode of the Ti:S laser. Then, the continuous frequency tuning of the 455 nm laser was implemented by scanning the length of the laser resonator by driving the PZT_1 and PZT_2 after locking the IE to the oscillating longitudinal mode of the laser. The experimental result was shown in Fig. 4. The continuous tuning range can reach up to 16 and 32 GHz while mode hop free for the FW laser and second-harmonic wave blue laser, respectively.

Eventually, to further prove the practicability of the achieved blue laser for the higher state excitation transition ($6^2S_{1/2} \leftrightarrow 7^2P_{3/2}$) of Cs atoms, a small part of the blue beam was separated from the main beam by a prism and an HWP and injected into a measurement system of 455 nm Cs atom saturation spectroscopy, which included four flat high reflectors (M_8, M_9, M_{10}, M_{11}), a Cs vapor cell, two neutral density filters (NDF_1 and NDF_2), and a balanced zero-beat detector PD_2, as shown in Fig. 5. M_8 was a special beam splitter with a thickness of 9 mm, which can leak a strong blue laser beam I_1 as the pump beam and reflect two weak blue laser beams from both surfaces as the probe beam I_2 and reference beam I_3 with the approximately same intensity, respectively. The probe laser beam I_2 and leaked pump laser beam I_1 were aligned by M_9, M_{10}, and M_{11} and simultaneously passed though the absorbing sample cell filled with Cs atom gas from opposite directions to ensure the probe laser beam I_2 to pass through the saturated region of the Cs cell by the pump laser beam I_1. The reference laser beam I_3 directly passed through the unsaturated region of

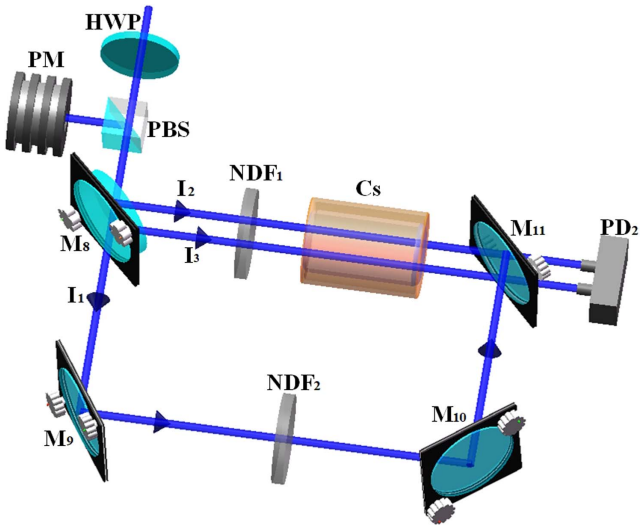

Fig. 5. Experimental setup for saturation spectroscopy of Cs.

the Cs cell. The Cs cell was a cylindrical glass cell with a length of 7.5 cm and a diameter of 2.5 cm. It can be heated from room temperature to 150°C by using the temperature control circuit. The leaked probe beam and the reference beam from the M_{11} were detected by the balanced zero-beat detector PD_2. The Doppler-broadened background can be successfully eliminated, and the Doppler-free spectral signal can be measured. When the temperature of the Cs cell was controlled at 90°C and the frequency of the blue laser was continuously scanned over 17.7 GHz, the desired whole SAP of Cs higher state hyperfine transitions of $6^2S_{1/2}(F_g = 3) \leftrightarrow 7^2P_{3/2}(F_e = 2, 3, 4)$ and $6^2S_{1/2}(F_g = 4) \leftrightarrow 7^2P_{3/2}(F_e = 3, 4, 5)$ near 455.528 nm were successfully obtained, which is illustrated in Fig. 6.

Figure 6(a) shows the energy levels of the 455 nm transitions related to the spectral signal [12]. It was clear that there were two and four hyperfine levels for ground and excited states, respectively. Figure 6(b) shows the measured two-saturation spectra with a frequency difference of 9.193 GHz, which was consistent with the energy levels of the Cs atoms shown in Fig. 6(a). Subtracting the reference laser beam I_3 with the saturated probe laser beam, the hyperfine transitions of two saturation spectra depicted in Fig. 6(b) can further experimentally observed, which are shown in Figs. 6(c) and 6(d). Figure 6(c) was corresponding to the principal and crossover lines of $F_g = 4 \leftrightarrow F_e = 3$, $F_g = 4 \leftrightarrow F_e = 3, 4$, $F_g = 4 \leftrightarrow F_e = 4$, $F_g = 4 \leftrightarrow F_e = 3, 5$, $F_g = 4 \leftrightarrow F_e = 4, 5$, and $F_g = 4 \leftrightarrow F_e = 5$. Figure 6(d) was corresponding to the principal and crossover lines of $F_g = 3 \leftrightarrow F_e = 2$, $F_g = 3 \leftrightarrow F_e = 2, 3$, $F_g = 3 \leftrightarrow F_e = 3$, $F_g = 3 \leftrightarrow F_e = 2, 4$, $F_g = 3 \leftrightarrow F_e = 3, 4$, and $F_g = 3 \leftrightarrow F_e = 4$.

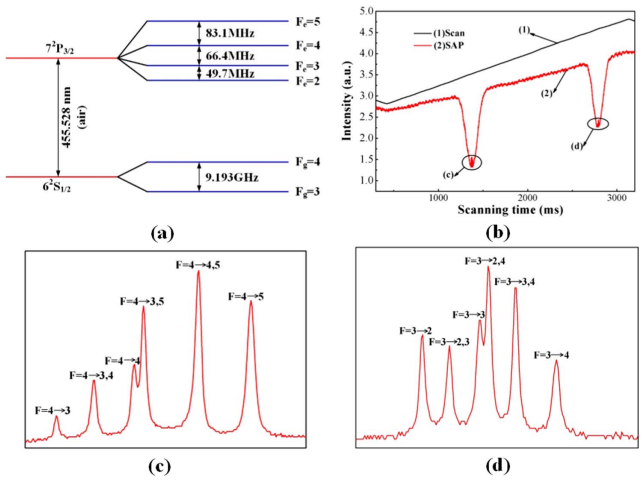

Fig. 6. (a) Relative energy levels of Cs and their frequency differences, (b) the saturation absorption spectrum of Cs, (c) the transitions peaks corresponding to $6^2S_{1/2}(F_g = 4) \leftrightarrow 7^2P_{3/2}(F_e = 3, 4, 5)$, and (d) the transitions peaks corresponding to $6^2S_{1/2}(F_g = 3) \leftrightarrow 7^2P_{3/2}(F_e = 2, 3, 4)$.

In summary, we realized a continuously tunable single-frequency 455 nm blue laser for high-state excitation transition of Cs atoms by a frequency-doubled Ti:S laser. The output power of 1.0 W was attained under the pump power of 13.5 W with the optical conversion efficiency of 7.4%. The measured power stability in 3 h and beam quality were better than ±0.27% (peak-to-peak) and $M_x^2 = 1.58$, $M_y^2 = 1.18$, respectively. A direct modulation-locking technology was adopted to lock the IE for realizing the continuous frequency tuning of the 455 nm blue laser. In this case, the continuous tuning range of CW 455 nm blue light was up to 32 GHz and was mode hop free. At last, using the obtained tunable 455 nm blue laser, the whole SAP of Cs higher state hyperfine transitions of $6^2S_{1/2}(F_g = 4) \leftrightarrow 7^2P_{3/2}(F_e = 3, 4, 5)$ and $6^2S_{1/2}(F_g = 3) \leftrightarrow 7^2P_{3/2}(F_e = 2, 3, 4)$ near 455.528 nm was obtained. The experimental results revealed that the attained tunable 455 nm laser can be used in further experiments of an atom light coupled system in quantum optics. Especially, the 455.5 nm light source with high output power was quite significant for ARFs and remote sensing in the deep sea communication.

Funding. National Key R&D Program of China (2016YFA0301401); Shanxi "1331 Project" Key Subjects Construction.

REFERENCES

1. T. Dutta, D. D. Munshi, D. Yum, R. Rebhi, and M. Mukherjee, Sci. Rep. **6**, 29772 (2016).
2. C. Auchter, T. W. Noel, M. R. Hoffman, S. R. Williams, and B. B. Blinov, Phys. Rev. A **90**, 060501 (2014).
3. J. T. Schultz, S. Abend, D. Doring, J. E. Debs, P. A. Altin, J. D. White, N. P. Robins, and J. D. Close, Opt. Lett. **34**, 2321 (2009).
4. M. Auzinsh, R. Ferber, F. Gahbauer, A. Jarmola, L. Kalvans, and A. Atvars, Opt. Commun. **284**, 2863 (2011).
5. Y. F. Wang, X. G. Zhang, D. Y. Wang, Z. M. Tao, Z. Wei, and J. B. Chen, Opt. Express **20**, 25817 (2012).
6. M. Schmidt, E. Heumann, C. Czeranowsky, and G. Huber, in *Conference on Lasers and Electro-Optics*, OSA Technical Digest (2001), paper CThC1
7. https://www.toptica.com/products/tunable-diode-lasers/ecdl-dfb-lasers/dl-pro/
8. L. S. Cruz and F. C. Cruz, Opt. Express **15**, 11913 (2007).
9. F. Q. Li, H. J. Li, and H. D. Lu, IEEE J. Quantum Electron. **52**, 1700106 (2016).
10. H. D. Lu and K. C. Peng, Acta Sin. Quantum Opt. **21**, 171 (2015).
11. Q. W. Yin, H. D. Lu, J. Su, and K. C. Peng, Opt. Lett. **41**, 2033 (2016).
12. D. Y. Wang, Y. F. Wang, Z. M. Tao, S. N. Zhang, Y. L. Hong, W. Zhuang, and J. B. Chen, Chin. Phys. Lett. **30**, 060601 (2013).

218.26.34.77 {ts '2019-10-12 03:40:48'}